

Project No. 09-782

# Computational Design of Advanced Nuclear Fuels

---

## Fuel Cycle R&D

Dr. Sergey Savrasov  
University of California Davis

In collaboration with:  
Rutgers University

Frank Goldner, Federal POC  
Cetin Unal, Technical POC

## NEUP PROJECT FINAL REPORT

**Project Title:** Computational Design of Advanced Nuclear Fuels

**Covering Period:** October 1, 2009 through September 30, 2013

**Date of Report:** May 28, 2014

**Recipient:** University of California Davis  
One Shields Ave  
Davis, CA 95616

**Award Number:** TBD

**Project Number:** 09-782

**Principal Investigator:** Sergey Savrasov  
Phone: 530-9026391  
Email: [savrasov@physics.ucdavis.edu](mailto:savrasov@physics.ucdavis.edu)

**Collaborators:** Gabriel Kotliar, Rutgers University, [kotliar@physics.rutgers.edu](mailto:kotliar@physics.rutgers.edu)  
Kristjan Haule, Rutgers University, [haule@physics.rutgers.edu](mailto:haule@physics.rutgers.edu)

# I. PROJECT OVERVIEW

## ***Objective:***

The objective of the project was to develop a method for theoretical understanding of nuclear fuel materials whose physical and thermophysical properties can be predicted from first principles using a novel dynamical mean field method for electronic structure calculations. We concentrated our study on uranium, plutonium, their oxides, nitrides, carbides, as well as some rare earth materials whose 4f electrons provide a simplified framework for understanding complex behavior of the f electrons. We addressed the issues connected to the electronic structure, lattice instabilities, phonon and magnon dynamics as well as thermal conductivity. This allowed us to evaluate characteristics of advanced nuclear fuel systems using computer based simulations and avoid costly experiments.

## ***Background:***

Actinide compounds display rich and complex physics which is the result of a great number of competing interactions in the microscopic Hamiltonian. The complexity primarily arises from a greater spatial extent of the actinide 5f orbitals which makes the f electrons display very different degree of localization in different compounds. For example, 5f electrons can be found in a well localized quasi-ionic regime (e.g.  $\text{UO}_2$ ,  $\text{PuO}_2$ ), a partially delocalized Kondo fluctuating regime ( $\text{UTe}$  or  $\text{NpSn}_3$ ), a mixed valence regime (e.g.  $\text{PuS}$  or  $\text{PuSe}$ ), or a fully itinerant regime, i.e. when the 5f electrons contribute fully to the volume of the Fermi surface and the bonding (e.g.  $\alpha$  Pu).

In this project we concentrated on a class of systems relevant for the design of nuclear fuels. These are at first place uranium, plutonium, their oxides, nitrides and carbides as well as their mixtures with fission product elements such, e.g., as Np, Cm, Am. We addressed the issues connected to their lattice instabilities, phonon and magnon dynamics as well as thermal conductivity. Building a robust theory to predict the complex behavior of these materials has a great potential for future computational design of advanced nuclear energy systems via computer simulations of phase diagrams, structural stability, lattice dynamics, magnetic, transport and spectroscopic properties of many promising actinide compounds. Our main objective was to develop a set of novel computational tools capable of fully treating the complex character of the *f*-electrons and to apply this method to study electronic, magnetic and lattice properties of the actinides.

We have recently developed a novel electronic structure method based on Dynamical Mean Field Theory (DMFT) capable of describing materials near the Mott transition. Based on this method, we have recently argued that the huge volume expansion in metallic Pu is the manifestation of the competition between the localization (caused by the electron-electron interactions) and delocalization (caused by the kinetic energy) tendencies. Our advances in understanding the electronic structure of the actinides have recently translated into predictions of the vibrational and elastic properties of this metal.

As an example of successes of this approach, we mention our recent successful prediction of the phonon spectra of delta Plutonium which was later confirmed experimentally by an inelastic X-ray scattering measurements by a team based at LLNL. Related experimental studies have been also carried out at LANL. Very recently, our theoretical developments have allowed us to look at various atomic states of Plutonium and Curium metals to uncover the valence of actinides and explain from a unified framework why some actinides, such as Curium, are magnetic and other, like Plutonium, are not. As another most recent example, we have predicted lattice dynamical properties of  $\text{UO}_2$  and  $\text{PuO}_2$  and uncovered various contributions to their thermal conductivities via calculated Grüneisen constants. These applications open new ways for exploring the performance of advanced nuclear fuels via computer based simulations.

### ***Products:***

We have developed a variety of computational algorithms and codes that allow us to simulate properties of systems with unfilled f electron shells. These include the following developments:

- 1. *Computer codes implementing LDA+DMFT using Kondo impurity solver:*** This set of codes was implemented by Munehisa Matsumoto, our postdoc supported by this award, and includes self-consistent implementation of a combination of local density approximation and dynamical mean field theory where instead of full solution of Anderson impurity problem, a simplified Kondo impurity problem is solved using a Continuous Time Quantum Monte Carlo Method. This code has been tested on a variety of Cerium and Plutonium based heavy fermion compounds as highlighted in project publications **1** and **2**.
- 2. *Computer codes for electron-phonon interactions in relativistic systems:*** This set of codes was implemented by Quan Yin, our postdoc supported by this award, and includes calculations of phonons and electron-phonon interactions that include both relativistic and strong correlation effects. We have tested a variety of nuclear fuel materials, such as Uranium, Plutonium, Americium oxides, carbides, nitrides using this computer code as highlighted in project publication **3**.
- 3. *Computer codes for relativistic GW Method:*** This set of codes was implemented by Andrey Kutepov, our postdoc supported by this award, and includes self-consistent implementation of relativistic GW method for electronic structure calculations of actinide materials. The code was benchmarked on elemental Plutonium and Americium metals as highlighted in project publication **4**.
- 4. *Computer codes for multipolar exchange interactions:*** This set of codes was implemented by Shu-Ting Pi, our student supported by this award, and includes evaluations of anisotropic exchange interactions between general multipolar moments that appear in relativistic materials with unfilled f-shells. The code was benchmarked on computing magnon spectrum for  $\text{UO}_2$  as highlighted in publications **6** and **8**.

**5. Computer codes for LDA+G method:** This set of codes was implemented by our student Ruanchen Dong, supported by this award, and includes self-consistent implementation of a combination of local density approximation with many body Gutzwiller method for electronic structure calculations of quasiparticles mass renormalizations in f electron materials. The code was benchmarked on several models and a variety of Cerium based heavy-fermion materials as highlighted in publications **5** and **7**.

**6. Computer codes for temperature-dependent parameterization of embedded-atom method:** This set of codes was implemented by our student Quan Yin, supported by this award, and includes a phenomenological temperature-dependent parameterization of the embedded-atom method combined with molecular dynamics to simulate the diverse physical properties of elemental plutonium. The new model captures its negative thermal expansion and strong temperature dependence of the bulk modulus as highlighted in publication **9**.

## II. PUBLICATIONS

### *Journal Papers*

**1.** Munehisa Matsumoto, Myung Joon Han, Junya Otsuki, and Sergey Yu. Savrasov  
Magnetic quantum critical point and dimensionality trend in cerium-based heavy-fermion compounds.

Physical Review B **82**, 180515 (2010) Rapid Communication

**2.** Munehisa Matsumoto, Quan Yin, Junya Otsuki, and Sergey Y. Savrasov  
Multiple quantum phase transitions of plutonium compounds.

Physical Review B **84**, 041105 (2011) Rapid Communication

**3.** Quan Yin, Andrey Kutepov, Kristjan Haule, Gabriel Kotliar, Sergey Y. Savrasov, and W. E. Pickett, Electronic correlation and transport properties of nuclear fuel materials.

Physical Review B **84**, 195111 (2011).

**4.** Andrey Kutepov, Kristjan Haule, Sergey Y. Savrasov, and Gabriel Kotliar  
Electronic structure of Pu and Am metals by self-consistent relativistic GW method.

Physical Review B **85**, 155129 (2012).

**5.** R. Dong, J. Otsuki, and S. Y. Savrasov  
Scaling between periodic Anderson and Kondo lattice models.

Physical Review B **87**, 155106 (2013).

**6.** Shu-Ting Pi, Ravindra Nanguneri and Sergey Savrasov  
Calculation of Multipolar Exchange Interactions in Spin-Orbital Coupled Systems.

Physical Review Letters **112**, 077203 (2014).

7. Ruanchen Dong, Xiangang Wan, Xi Dai, Sergey Y. Savrasov  
Orbital Dependent Electronic Masses in Ce Heavy Fermion Materials studied via  
Gutzwiller Density Functional Theory.  
Physical Review B **89**, 165122 (2014).

8. Shu-Ting Pi, Ravindra Nanguneri and Sergey Savrasov  
Anisotropic Multipolar Exchange Interactions in Systems with Strong Spin-Orbit  
Coupling.  
arXiv:1406.0221 (submitted to Physical Review B)

9. Z. P. Yin, Xiaoyu, Deng, K. Basu, Q. Yin, and G. Kotliar  
Temperature dependent electronic structures, atomistic modeling and the negative  
thermal expansion of Pu.  
arXiv:1303.3322 (Philosophical Magazine Letters, in press, 2014).

### ***Conference Papers and Invited Talks:***

1. Invited Talk at Lawrence Livermore National Laboratory, October 2009  
Sergey Savrasov, University of California Davis  
Recent Advances in Studying Electronic Structure of Actinides and Heavy Fermion  
Systems

2. Invited Talk at American Chemical Society Meeting, San Francisco, California, March  
2010  
Sergey Savrasov, University of California Davis  
Recent Advances in Studying Electronic Structure of Actinides

3. March Meeting of the American Physical Society, Portland, OR, USA, 2010  
Quan Yin, Sergey Savrasov, Warren Pickett  
B38.00015 : Correlated Electronic Structures of Actinide Compounds

4. Condensed Matter Seminar at University of California Davis, April 2010  
Munehisa Matsumoto, University of California Davis  
Plutonium compounds as Kondo lattices in the strong coupling limit

5. Condensed Matter Seminar at University of California Los Angeles, May 2010  
Sergey Savrasov, University of California Davis  
Recent Advances in Studying Actinides and Heavy Fermion Systems using LDA+DMFT

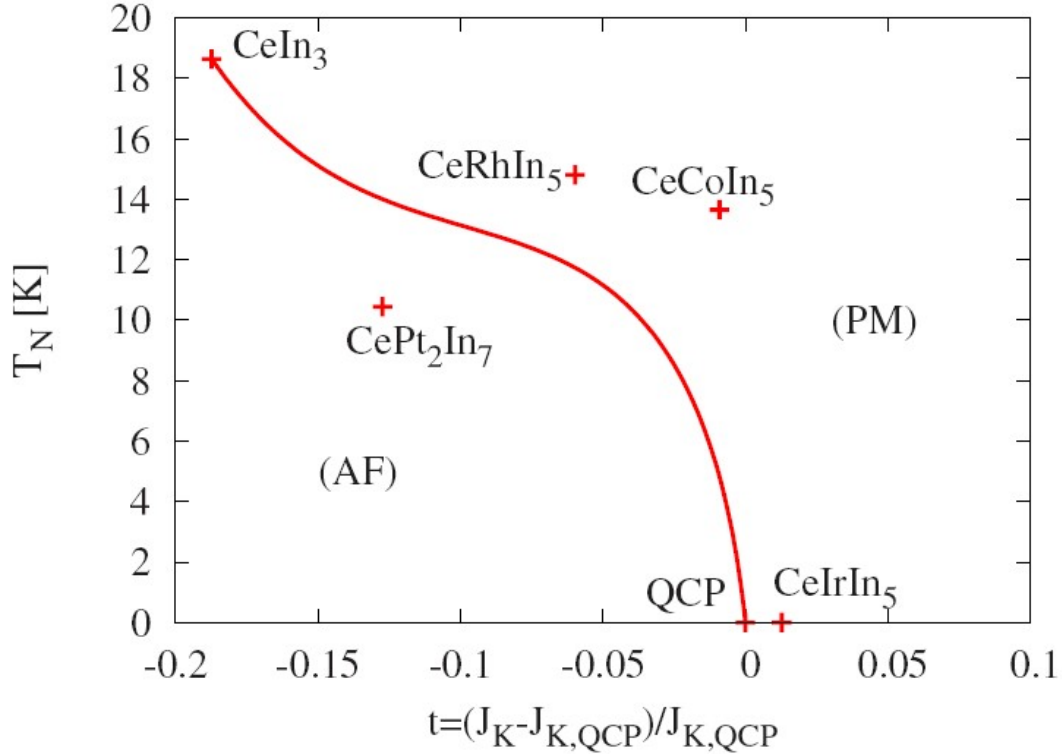
6. ICAM Workshop on Novel Energy Materials, Beijing, June 2010  
Sergey Savrasov, University of California Davis  
Nuclear Fuels as Strongly Correlated Systems

7. March Meeting of the American Physical Society, Boston, Massachusetts, USA, 2011  
Munehisa Matsumoto, Sergey Savrasov, Junya Otsuki  
S1.00274 : Predicting Sommerfeld coefficients for heavy-fermion materials
8. March Meeting of the American Physical Society, Boston, Massachusetts, USA, 2011  
Quan Yin, Kristjan Haule, Gabriel Kotliar, Sergey Savrasov, Warren Pickett  
W31.00003 : Electron Correlation and Transport Properties in Nuclear Fuel Materials
9. Condensed Matter Seminar at Max-Planck Institute for Solid State Research, Stuttgart, February 2012  
Sergey Savrasov, University of California Davis  
Nuclear Fuels as Strongly Correlated Systems
10. Condensed Matter Seminar at University of California Berkeley, May 2012  
Sergey Savrasov, University of California Davis  
Nuclear Fuels as Strongly Correlated Systems
11. NEUP Presentation at University of California Davis, January 2013  
Sergey Savrasov, University of California Davis  
Computational Design of Advanced Nuclear Fuels
12. Annual Meeting of the California-Nevada Section of the APS, Rohnert Park, CA, November 2013  
Shu-Ting Pi, Ravindra Nanguneri, Sergey Savrasov  
D2.00007 : Calculation of Multipolar Exchange Interactions in Spin-Orbital Coupled Systems
13. March Meeting of the American Physical Society, Denver, CO, USA, 2014,  
W43.00010, Floquet Topological Insulators in Uranium Compounds  
Shu-Ting Pi, Sergey Y. Savrasov
14. Invited Talk at Plutonium Futures: The Science 2014, Las Vegas, NV, September 2014 (forthcoming)  
Sergey Savrasov, University of California Davis  
Computing Properties of Nuclear Fuels

### III. PROJECT TASKS

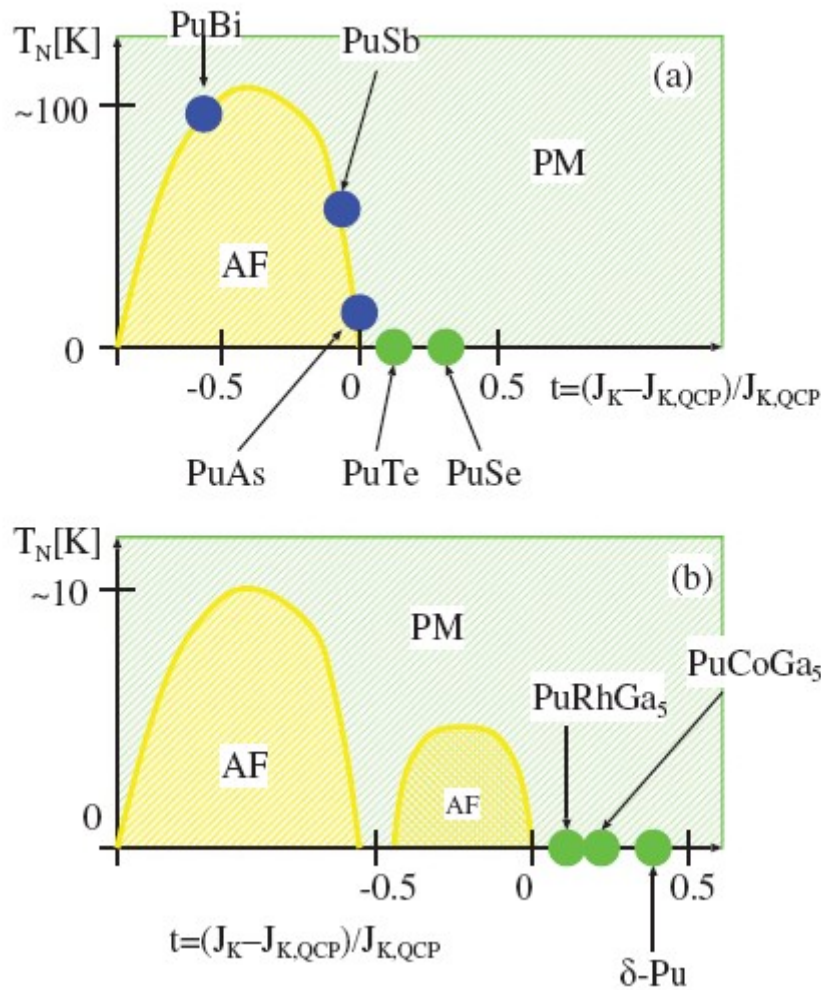
1. *Simulations for f-electron systems using a combination of density functional theory and Kondo impurity problem.* Here two classes of systems have been studied. First, magnetic quantum critical point and dimensionality trend in cerium-based heavy-fermion compounds has been investigated. It was based on realistic Kondo-lattice simulation results for the recently discovered heavy-fermion antiferromagnet CePt<sub>2</sub>In<sub>7</sub> and compared with its three-dimensional counterpart CeIn<sub>3</sub> and the less two-dimensional ones, Ce-115's. We found that the distance to the magnetic quantum critical point (QCP)

is the largest for CeIn<sub>3</sub> and the smallest for Ce-115's, and CePt<sub>2</sub>In<sub>7</sub> falls in between. We argued that the trend in quasi-two-dimensional materials stems from the frequency dependence of the hybridization between cerium 4f electrons and the conduction bands.



Our main result is summarized on the universal Doniach phase diagram for CePt<sub>2</sub>In<sub>7</sub>, and Ce-115's together with their parent compound, CeIn<sub>3</sub> with the horizontal axis rescaled to measure the distance to the magnetic quantum critical point. We inspect the distance to the QCP of CePt<sub>2</sub>In<sub>7</sub> referring to those of Ce-115's and CeIn<sub>3</sub>. The cubic parent material CeIn<sub>3</sub> is seen to be most separated from QCP and Ce-115's are found to be concentrated in the neighborhood to QCP, with CeRhIn<sub>5</sub> on the magnetic side and CeIrIn<sub>5</sub> on the nonmagnetic side. Our numerical resolution is not sufficient to locate CeCoIn<sub>5</sub> in its correct nonmagnetic side but it is clear that it sufficiently works to estimate the extreme closeness to QCP of Ce-115's. We note that our calculation scheme might not be as good for CeCoIn<sub>5</sub> as for the others due to the possibly stronger effects of valence fluctuations in this material. It is seen that when we try to reach the QCP from CeIn<sub>3</sub> in the three-dimensional limit, CePt<sub>2</sub>In<sub>7</sub> is located in the midway toward Ce-115's which are located closest to the QCP. Seen from QCP, CeIn<sub>3</sub> is already close enough to enable the pressure-driven superconductivity<sup>36</sup> and CePt<sub>2</sub>In<sub>7</sub> would also have one. Making a material more 2D indeed helps it to come closer to QCP, which is reasonable in the general context that the lower spatial dimensionality would suppress the magnetic long-range order. However, within the 2D side, the trend among CePt<sub>2</sub>In<sub>7</sub> and Ce-115's is somewhat nonmonotonic. On top of the spatial dimensionality, the frequency dependence of the hybridization seems to introduce the nontrivial trend in this way.

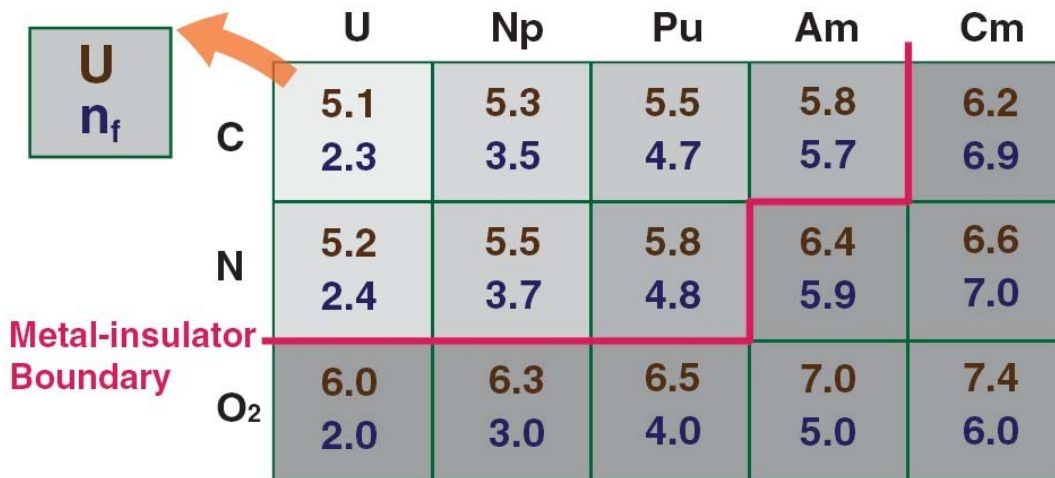
Second, we studied multiplicity of quantum phase transitions of plutonium compounds where we showed by quantum Monte Carlo simulations of realistic Kondo lattice models derived from electronic structure calculations that multiple quantum critical points can be realized in plutonium-based materials. We placed representative systems, including PuCoGa<sub>5</sub>, on a realistic Doniach phase diagram and identified the regions where the magnetically mediated superconductivity could occur. The solution of an inverse problem to restore the quasiparticle renormalization factor for  $f$  electrons was shown to be sufficiently good to predict the trends among Sommerfeld coefficients and magnetism. A suggestion on the possible experimental verification for this scenario was given for PuAs. Publications 1 and 2 have resulted from this research.



Schematic summary of our magnetic phase diagrams for Pu compounds is plotted here on the  $(t, T_N)$  plane, where  $t \equiv (J_K - J_{K,QCP}) / J_{K,QCP}$  is the rescaled Kondo coupling, with  $J_{K,QCP}$  being the first QCP in (a) and the third QCP in (b). A striking multidome structure shows up together with multiple QCP's for materials with strong Kondo coupling. We find that Pu-115's are located in a region where the antiferromagnetic long-range order is suppressed, possibly near a hidden or pseudo-QCP, within some numerical noise at the

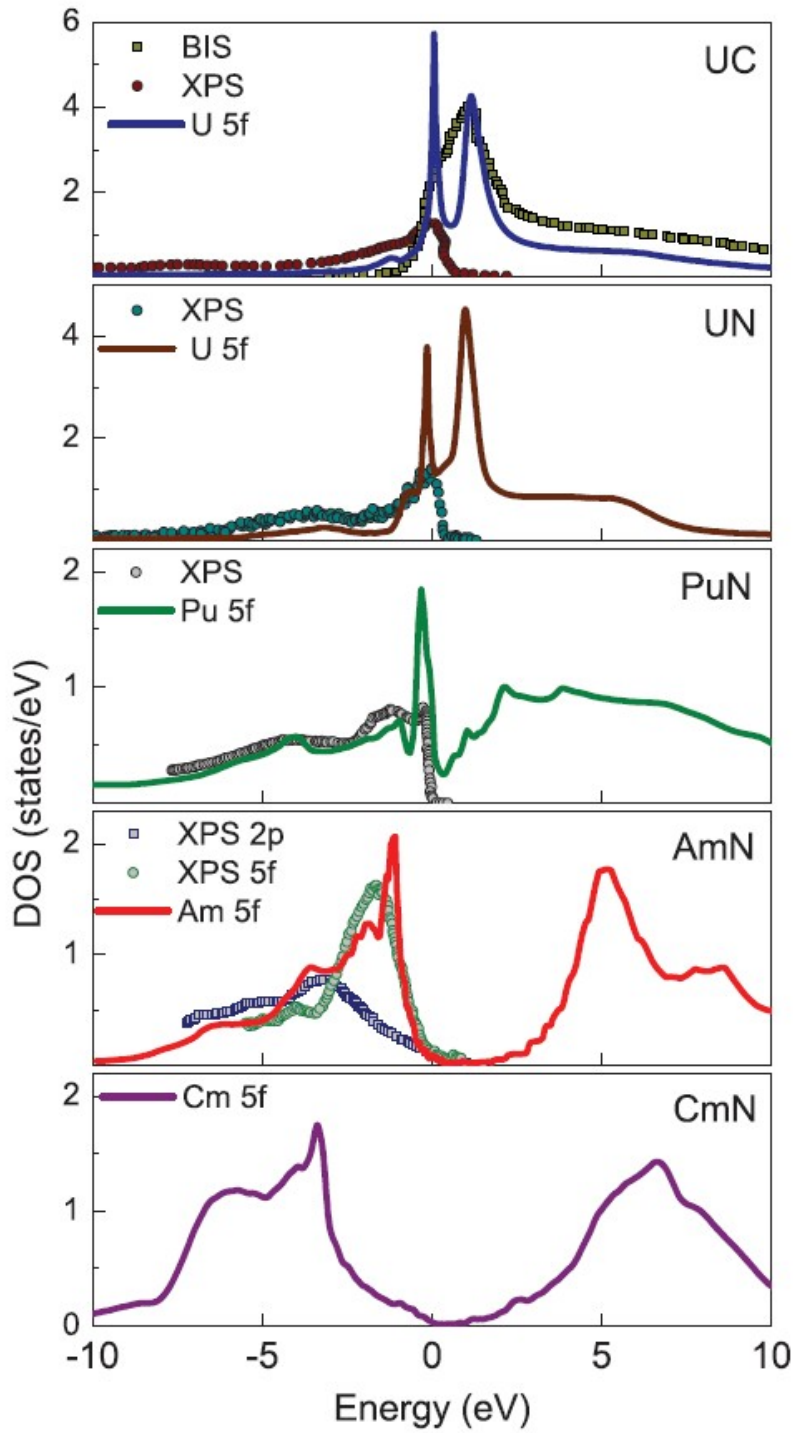
lowest reachable temperatures at present. Inspecting the distribution of materials around the QCP's in this figure, we have pnictides on the left-hand side and chalcogenides on the right-hand side of the antiferromagnetic QCP. This is consistent with what has been known experimentally; that is, pnictides, such as PuAs, PuSb, and PuBi, are magnets and chalcogenides, such as PuSe and PuTe, are paramagnets. The actual magnetism is strongly spatially anisotropic, and its treatment is unfortunately beyond the level of single-site DMFT description. For now, we will leave the issue of ordering wave vectors for future presentations and focus on the trends across target materials spanning between magnetism and HF behavior. The characteristic energy scales of Kondo screening and magnetic ordering have been captured by fully incorporating the frequency dependence of the hybridization.

**2. Studies of electronic correlation effects and transport properties in nuclear fuel materials.** The electronic structures and transport properties of a series of actinide monocarbides, mononitrides, and dioxides were studied systematically using a combination of density-functional theory and dynamical mean-field theory. The studied materials present different electronic correlation strength and degree of localization of  $5f$  electrons, where a metal-insulator boundary naturally lies within. In the spectral function of Mott-insulating uranium oxide, a resonance peak was observed in both theory and experiment and may be understood as a generalized Zhang-Rice state. We also investigated the interplay between electron-electron and electron-phonon interactions, both of which are responsible for the transport in the metallic compounds. Our findings allow us to gain insight in the roles played by different scattering mechanisms, and suggest how to improve their thermal conductivities. Publication 3 has resulted from this research.

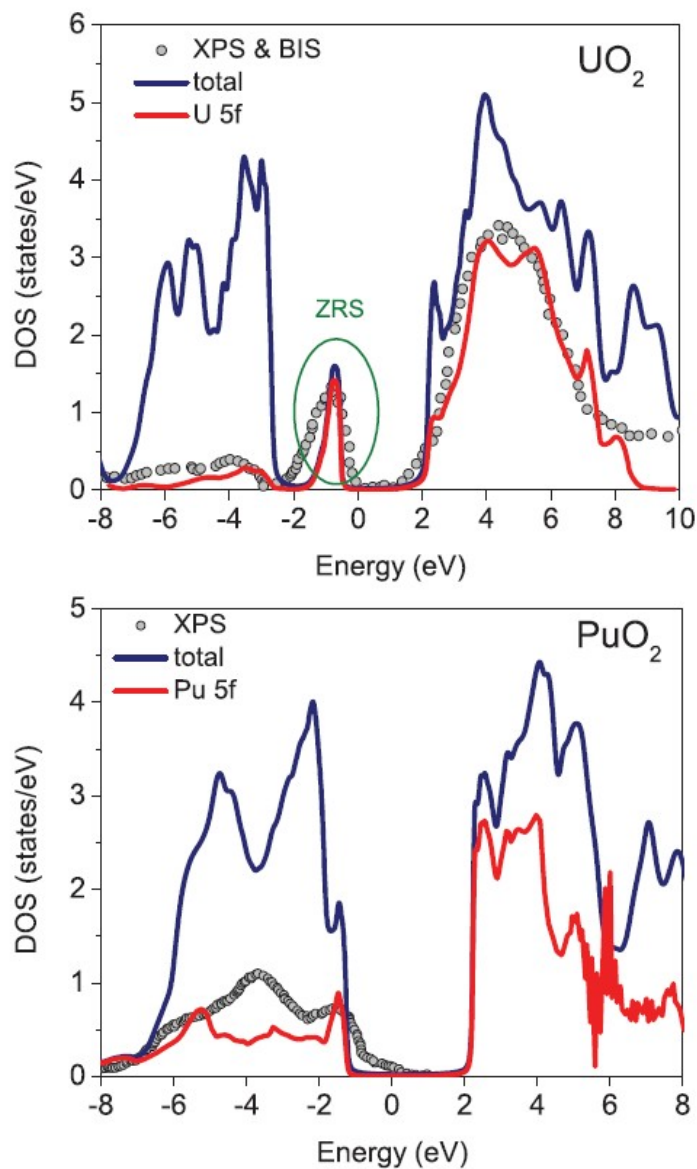


One of our major results is establishing proximity of nuclear fuel materials to metal-insulator transition which has resulted in the correlation phase diagram shown above. The overall correlation strength and localization is visualized by the shading on this figure, where the gray gradient approximately represents the partial  $f$  density of states at the Fermi level computed by LDA+DMFT. The labels on the top denote the actinide

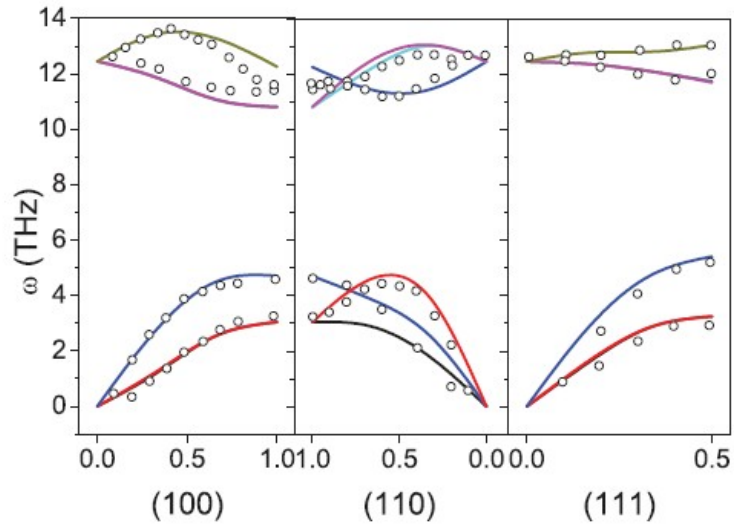
elements, and the labels to the left denote the ligand elements. The red line is the metal-insulator boundary. Two quantities, which are computed at  $T = 100$  K, are listed in each cell: Hubbard  $U$  (units: eV) and  $f$ -electron valence  $n_f$ .



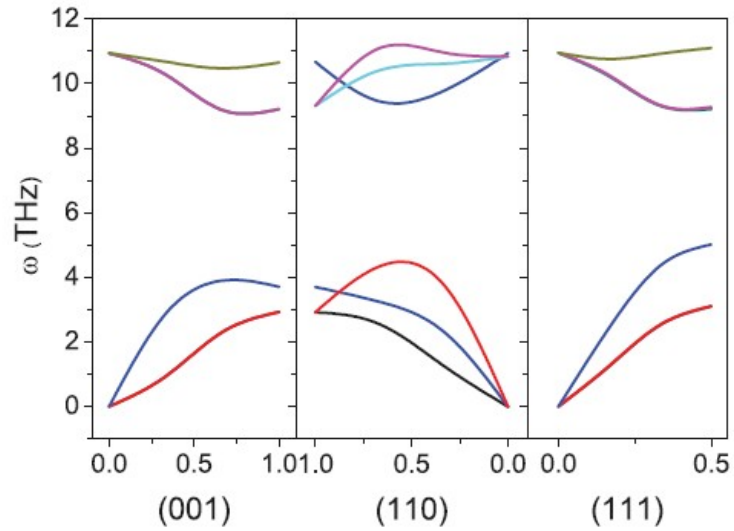
We presented the frequency dependence of the electronic spectral functions of some representative compounds in this figure. From the top panel to the bottom, the 5f partial density of states (DOS) changes qualitatively. UC and UN represent an itinerant 5f - electron system with most spectral weight on the Fermi level, but the picture starts to change at PuN, where the Kondo resonance and satellite 5f states are present. In AmN the 5f DOS begins to form an marginal energy gap. The evolution of the density of states from UN to CmN echoes the itinerancy-localization transition of 5f electrons, and demonstrates the metal-insulator transition in a transparent point of view. CmC, CmN, and all the actinide oxides are also found to be insulators. This allows us to establish a metal-insulator transition boundary, illustrated by the thick red line in our correlation phase diagram discussed earlier.



We now turn to the electronic structure of oxides. Hybrid functionals, especially the newly developed Heyd-Scuseria-Ernzerhof (HSE) variant, which mixes a certain amount of Hartree-Fock exact exchange potential with LDA/generalized gradient approximation (GGA) potentials, has successfully captured strong correlation effects and produced qualitatively correct spectral properties, energy gaps, and accurate optimal lattice constants in actinide oxides. However, in these studies the spin-orbit coupling was not considered and the calculations were done in either the ferromagnetic (FM) or antiferromagnetic (AFM) state. As a generalization to DFT by adding static Hartree-Fock mean-field approximation of electron interactions, the LDA+U is widely used for electronic structure calculation of strongly correlated materials, and has been applied on actinide oxides such as  $\text{UO}_2$ ,  $\text{NpO}_2$  and  $\text{PuO}_2$ . Although some calculated physical properties were improved over LDA, the LDA+U relies on magnetic ordering to get the correct energy gap, and it does not capture real atomic features nor quasiparticle bands, and thus fails in correlated metallic compounds. Our novel LDA+DMFT study does not require the magnetic ordering to obtain the Mott insulating gap. The total and partial DOS of  $\text{UO}_2$  and  $\text{PuO}_2$  calculated by LDA+DMFT are shown in figure above. Both are Mott insulators with well formed Hubbard bands and large correlation energy gaps. Most noticeably, the situation  $U > \Delta$  allows us to describe the insulating actinide oxides as charge-transfer Mott insulators, which is well known from late transition-metal oxides, for example NiO, the classical textbook example of strongly correlated systems. As it is known from cuprates, which are charge-transfer type Mott insulators, that the Zhang-Rice state (ZRSs) would appear as the low-energy resonance corresponding to the coupling of local moments of correlated electron orbitals to the hole induced by photoemission process on ligand orbitals. This ZRS concept has been generalized to other transition-metal oxides, since they have the same physics as cuprates. In the case of  $\text{UO}_2$ , the situation is very similar because it also has a charge-transfer energy gap, and there is a local magnetic moment on the U  $5f^2$  orbital due to the  $\Gamma_5$  triplet being its many-body ground state. On the other hand,  $\text{PuO}_2$  does not have the ZRS because its ground state of the  $5f^4$  shell is the  $\Gamma_1$  singlet, which has zero moment. Since Hubbard bands are of atomic nature, the position of the lower Hubbard band (LHB) is found numerically by computing the many-body excitation energy of the impurity problem of DMFT, i.e.,  $E(f^2) - E(f^1)$ . In the theoretical spectral function of  $\text{UO}_2$ , the LHB is located at about  $-4.3$  eV, which is broad and hybridized heavily with the O  $2p$  band. By performing the same calculation with other values of  $U$ , we found that this resonance peak is not sensitive to the choice of  $U$ , while the Hubbard bands shift proportionally to  $U$ .



(a)



(b)

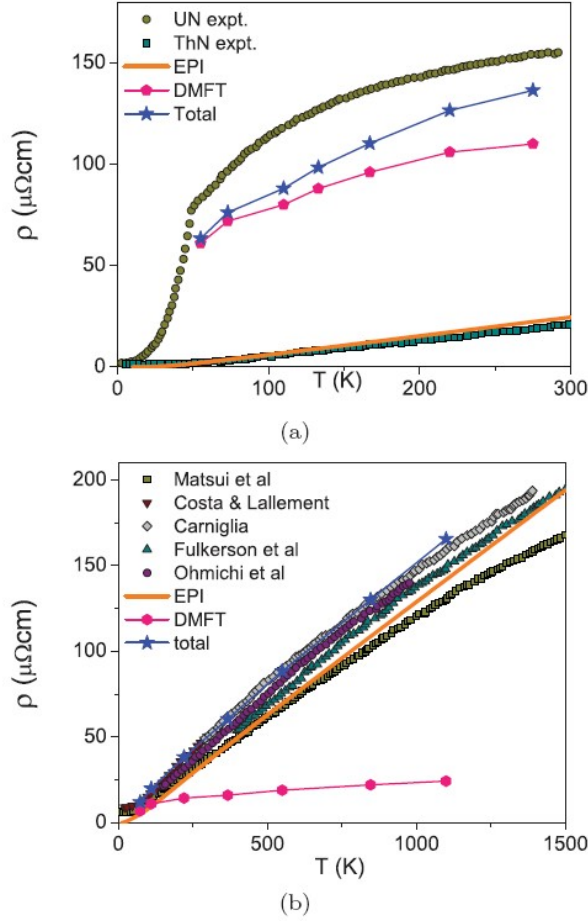
The phonon dispersion of UN along three high-symmetry directions is shown in figure (a) above together with experimental data measured by neutron scattering. As shown in (b), UC carries similar phonon dispersions but slightly lower phonon energies. Despite the apparent presence of correlation effects, excellent agreement is achieved with the local-density approximation (LDA). Similar success of LDA in studying lattice dynamics of strongly correlated metallic systems have been reported earlier, for example, in palladium, high-temperature superconducting cuprates, and recently iron pnictides.

Calculations of electron-phonon interactions and transport properties require quasiparticle description of the one-electron spectra when evaluating Eliashberg and transport spectral functions by integrating over the Fermi surfaces. As a result, due to large mass enhancement, the straightforward LDA procedure can produce wrong electron-phonon

resistivity, which was indeed found in our calculation for UC where  $\rho_{\text{EPI}}(T)$  was overestimated by a factor of 3 compared to experiment. This is despite of simple arguments that would suggest that any multiplicative effects on the electron mass renormalization should cancel out in the resistivity, because it enters both the scattering rate  $\tau$  that appears in the denominator, and the electronic mass that appears in the numerator of the expression for  $\rho_{\text{EPI}}(T)$ , which is evident from a simple Drude formula for  $\rho = m/(ne^2\tau)$ . However, in general, this does not apply to multiband systems where only correlated  $f$ -electron wave functions are primarily affected by strong Coulomb interactions.

In the present work we extend this method to compute electron-phonon interactions for systems such as UC and UN whose  $f$  electrons show itinerant behavior with  $m^*/m_{\text{LDA}} \approx 4\text{--}12$ . To capture this mass renormalization effect, we first make a fit to the self-energy obtained from the CTQMC, using a two-pole interpolation where the slope of the self-energy at zero frequency  $d\Sigma(\omega)/d\omega|_{\omega=0} = 1 - m^*/m_{\text{LDA}}$  controls the electronic mass enhancement while the positions of the self-energy poles determine the transfer of the spectral weight from the quasiparticle band to the Hubbard bands. Second, we assume that the  $f$  electrons are rigidly bound to their ions so that there is no actual change in the self-energy,  $\delta\Sigma(\omega)$ , caused by ionic excursions from their equilibrium positions. Since the main contribution to electronic transport comes from the states near the Fermi surface, where quasiparticles are best described in terms of slave bosons, the neglecting of  $\delta\Sigma(\omega)$  due to ion displacements corresponds to a rigid self-energy approximation. This is very similar to the famous rigid muffin tin approximation (RMTA), which has been successfully applied in the past to study electron-phonon interactions in transition-metal materials. Therefore our use of rigid selfenergy is expected to demonstrate a similar accuracy.

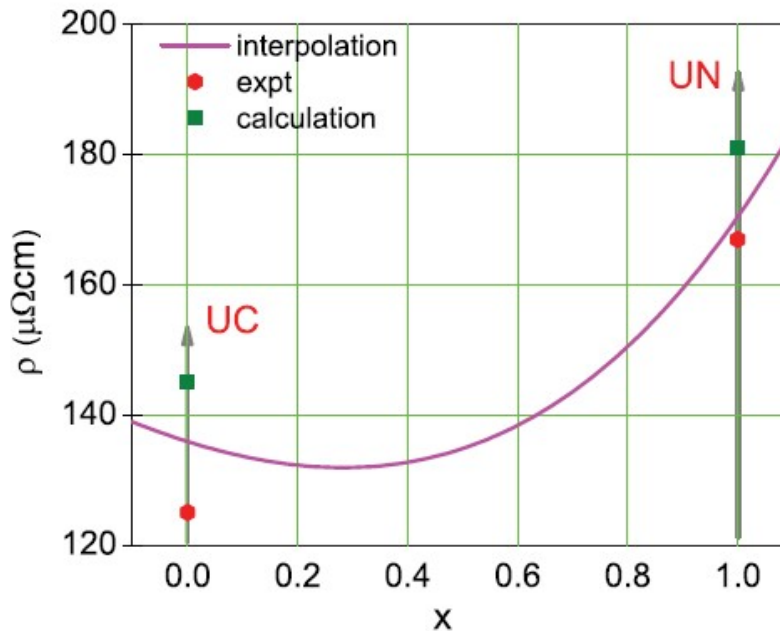
Since the inclusion of correlation effects also renormalizes bands and thus modifies the Fermi surface as well as the average electron velocity, the combined effect of electron correlation on  $\rho_{\text{EPI}}(T)$  is not straightforwardly seen. By applying this theory, we have obtained a substantial reduction (by a factor of 3) in  $\rho_{\text{EPI}}(T)$  for UC, while in UN the effect was marginal.



Taking into account both electron-electron and electron phonon scattering mechanisms, we can now build the entire picture of the electronic transport in the uranium compounds with our results summarized in this figure. Electron-electron scattering can account for approximately 80% of  $\rho(T)$  in UN, commonly found in heavy fermion systems, entitling it as a strongly correlated bad metal. In contrast, UC shows nearly linear  $\rho(T)$ , which is an indication of dominant electron phonon scattering, and our calculated results indeed show that in UC,  $\rho_{ee}(T)$  is much smaller than  $\rho_{\text{EPI}}(T)$ . The  $\rho_{\text{EPI}}(T)$  of UN shows very similar behavior, both qualitatively and quantitatively, to the experimental resistivity of ThN, which has no  $5f$  electrons and thus its resistivity is purely due to electron-phonon interaction. This comparison reflects the strong electron-electron correlation in UN, which acts as additional (and in this case major) scattering of electrons. Our calculations verify the distinct characters in the electrical transport of UC and UN, two seemingly similar materials. While electrical current can only be carried by electrons in solids, excitations other than electrons may contribute to thermal conductivity. Here we also estimate lattice vibrational contribution to thermal conductivity in UC and UN, using the phonon spectra we obtained from linear-response calculation. This is done by evaluating the Gruneisen parameter and phonon group velocities using our method that we developed previously for MOX fuels in Phys. Rev Lett. 103, 096403 (2009). According to our result, at  $T = 1000$  K, lattice thermal conductivity  $\kappa_{\text{ph}}$  is equal to 2.7 W/mK in UC, and  $\kappa_{\text{ph}} = 4.4$  W/mK in UN. Thus  $\kappa_{\text{ph}}$  only plays a minor role in these two metallic

uranium compounds. We put together our results and evaluate total thermal conductivity at 1000 K, a representative temperature under which nuclear reactors operate. By applying the Wiedemann-Franz law on the electrical conductivity data, we obtain  $\kappa_{ee}$ . Since electronic thermal resistivity consists of two scattering processes, total thermal conductivity is estimated by  $\kappa_{\text{total}} = (\kappa^{-1}_{ee} + \kappa^{-1}_{\text{EPI}})^{-1} + \kappa_{\text{ph}}$ , in which the first two terms correspond to  $\kappa_{\text{electron}}$ . For UN, our result,  $\kappa_{\text{total}} = 16.5$  W/mK, compares well with a recent study which extracted the phonon contribution from molecular dynamics (MD) and the electronic contribution from experiments. Experimentally,  $\kappa(1000 \text{ K}) \approx 19 - 23$  W/mK. In UC, we obtained  $\kappa_{\text{total}} = 18.7$  W/mK, also close to the experimental value of 23 W/mK. The discrepancy between theory and experiment is likely due to other excitations that can conduct heat but are not accounted for in our calculation, as well as the approximate nature of the Wiedemann-Franz law and Boltzmann transport theory, which are used to obtain the electronic and lattice thermal conductivity, respectively.

At last, the understanding gained from our computational study suggests avenues for improving the thermal conductivity of UC and UN. At high temperatures under which reactors operate, optimizing thermal conductivity is equivalent to minimizing resistivity. We investigate the doping dependence of the resistivity of the solid solution  $\text{UC}_{1-x}\text{N}_x$ . Here we explain how  $\text{UC}_{1-x}\text{N}_x$  solid solution can have smaller resistivity than the stoichiometric compounds, by using a set of simple interpolative equations to simulate the transport in the solid solution. Using the quantities obtained from our LDA+DMFT and linear-response calculations for the two end points of the solution (UC and UN), we can plot the interpolated  $\rho_{\text{total}}(T)$  as a function of  $x$ . In Figure below, it is clearly seen that a minimum exists. It is also possible to achieve similar effects in UC by electron doping, or in UN by hole doping.



**3. Studies of Electronic structures for Pu and Am metals by self-consistent relativistic  $GW$  method.** We presented the results of calculations for Pu and Am performed using an implementation of a self-consistent fully relativistic  $GW$  method. The key feature of our scheme is to evaluate polarizability and self-energy in real space and Matsubara's time. We compared our  $GW$  results with the calculations using local density and quasiparticle approximations and also with scalar-relativistic calculations. We highlighted the importance of both relativistic effects and effects of self-consistency in  $GW$  calculation for Am and Pu. We also have found that  $GW$  enhances the hybridization between  $5f$  and  $6d$  states in Pu, suggesting that the physics of Pu should not be understood based only on  $5f$  electrons. Publication 4 has resulted from this research.

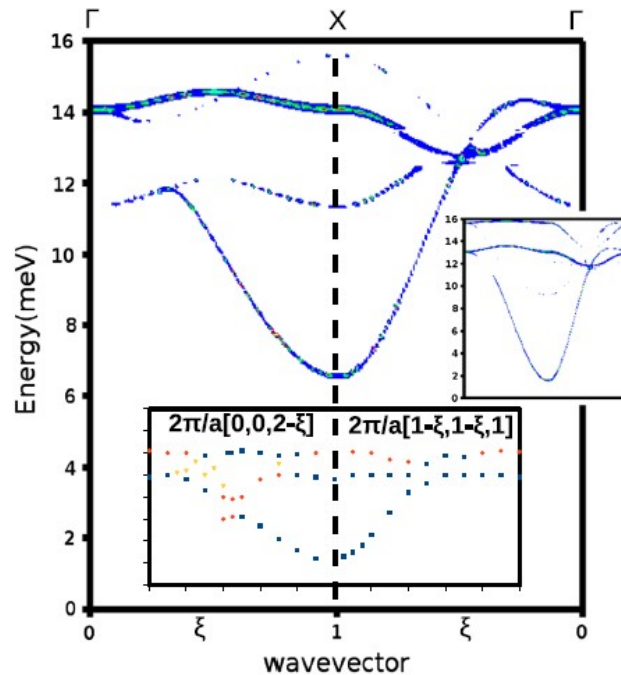
**4. Developments of combined LDA and Gutzwiller Methods for  $f$ -electron systems.** We first studied scaling between periodic Anderson and Kondo lattice models using Continuous-time quantum Monte Carlo method combined with dynamical mean field theory and calculated both periodic Anderson model (PAM) and Kondo lattice model (KLM). Different parameter sets of both models are connected by the Schrieffer-Wolff transformation. For degeneracy  $N = 2$ , a special particle-hole symmetric case of PAM at half filling which always fixes one electron per impurity site was compared with the results of the KLM. We found a good mapping between PAM and KLM in the limit of large on-site Hubbard interaction  $U$  for different properties like self-energy, quasiparticle residue and susceptibility. This allowed us to extract quasiparticle mass renormalizations for the  $f$  electrons directly from KLM. The method was further applied to higher degenerate case and to realistic heavy fermion system CeRhIn5 in which the estimate of the Sommerfeld coefficient is proven to be close to the experimental value. At the second stage of this task, we studied orbital-dependent electronic masses in Ce heavy-fermion materials via Gutzwiller density-functional theory. Computed orbital-dependent electronic mass enhancement parameters were compared with available experimental data extracted from measured values of the Sommerfeld coefficient. Gutzwiller density functional theory was shown to remarkably follow the trends across a variety of Ce compounds and to give important insights into the phenomenon of orbital-selective mass renormalization which in turn allows for a better understanding of a wide spread of data. Publications 5 and 7 have resulted from this research.

	$N_{\text{LDA}}(0)$ St./Ry cell	$\gamma_{\text{LDA}}$ mJ/(mol K <sup>2</sup> )	$\gamma_{\text{expt}}$ mJ/(mol K <sup>2</sup> )	Ref. to $\gamma_{\text{expt}}$	$z_{\text{expt}}$	$\gamma_{\text{LDA+G}}$ ( $U = 4$ eV)	$\gamma_{\text{LDA+G}}$ ( $U = 5$ eV)	$z_{\text{LDA+G}}$ ( $U = 4$ eV)	$z_{\text{LDA+G}}$ ( $U = 5$ eV)	Orbital $j = 5/2$
$\alpha$ Ce	36	6.2	13	[3]	0.48			0.55	0.33	$\Gamma_7, \Gamma_8$
$\gamma$ Ce	49	8.5						0.14	0.11	$\Gamma_7, \Gamma_8$
115s:										
CeCoIn <sub>5</sub>	150	26.0	290	[6]	0.09	70	104	0.20	0.13	$\Gamma_6, 2\Gamma_7$
CeRhIn <sub>5</sub>	156	27.2	420	[7]	0.065	75	120	0.19	0.12	$\Gamma_6, 2\Gamma_7$
CeIrIn <sub>5</sub>	165	28.6	720	[8]	0.04	79	210	0.14	0.07	$\Gamma_6, 2\Gamma_7$
122s:										
CeMn <sub>2</sub> Si <sub>2</sub>	184	31.9	47	[9]	0.68	52	84	0.51	0.43	$\Gamma_6, 2\Gamma_7$
CeFe <sub>2</sub> Si <sub>2</sub>	85	14.7	22	[10]	0.67	21	24	0.53	0.47	$\Gamma_6, 2\Gamma_7$
CeCo <sub>2</sub> Si <sub>2</sub>	110	19.0	10	[11]	1.9?	35	43	0.47	0.36	$\Gamma_6, 2\Gamma_7$
CeNi <sub>2</sub> Si <sub>2</sub>	115	19.9	33	[12]	0.60	27	29	0.47	0.43	$\Gamma_6, 2\Gamma_7$
CeCu <sub>2</sub> Si <sub>2</sub>	64	11.1	1000	[13–15]	0.01	430	$\infty$	0.10	0	$\Gamma_6$
CeRu <sub>2</sub> Si <sub>2</sub>	103	17.8	350	[16–18]	0.05	70	190	0.33	0.13	$2\Gamma_7$
CeRh <sub>2</sub> Si <sub>2</sub>	106	18.3	130	[19]	0.14	35	120	0.36	0.14	$2\Gamma_7$
CePd <sub>2</sub> Si <sub>2</sub>	100	17.3	65–110	[20,21]	0.15–0.26	170	$\infty$	0.045	0	$\Gamma_7$
CeAg <sub>2</sub> Si <sub>2</sub>	205	35.5				140	430	0.10	0.06	$\Gamma_6$

The table above gives the summary of this task where we show the Comparison between calculated using LDA density of states and experimentally extracted specific heat coefficients  $\gamma$  and the extracted quasiparticle residues  $z_{\text{expt}} = \gamma_{\text{LDA}}/\gamma_{\text{expt}}$  for a number of cerium-based heavy-fermion compounds considered in this work. The last columns show the predictions of  $\gamma$  and  $z$  using the LDA + G method with the values of  $U = 4$  and  $5$  eV as well as the reference to the specific orbital degeneracy of the  $j = 5/2$  manifold that exhibits the strongest enhancement.

### 5. Calculations of Multipolar Exchange Interactions in Spin-Orbital Coupled Systems.

We introduced a theoretical framework for computations of anisotropic multipolar exchange interactions found in many spin-orbit coupled magnetic systems and proposed a method to extract these coupling constants using a density functional total energy calculation. This method was developed using a multipolar expansion of local density matrices for correlated orbitals that are responsible for magnetic degrees of freedom. Within the mean-field approximation, we showed that each coupling constant can be recovered from a series of total energy calculations via what we called the "pair-flip" technique. This technique flips the relative phase of a pair of multipoles and computes corresponding total energy cost associated with the given exchange constant. To test it, we applied our method to Uranium Dioxide, which is a system known to have pseudospin  $J=1$  superexchange induced dipolar, and superexchange plus spin-lattice induced quadrupolar orderings. Our calculation revealed that the superexchange and spin-lattice contributions to the quadrupolar exchange interactions are about the same order with ferro- and antiferro-magnetic contributions, respectively. This highlighted a competition rather than a cooperation between them. Our method could be a promising tool to explore magnetic properties of rare-earth compounds and hidden-order materials. Publications 6 and 8 have resulted from this research.



The figure above illustrates how we have obtained magnetic excitation of  $\text{UO}_2$  along two symmetry directions calculated by scanning the color map of the real part two-ion susceptibility of our Hamiltonian with parameters that we computed. Right inset: The same calculation made by requiring the overall quadrupole coupling to have 3-k symmetry. Anisotropy gap is greatly reduced. Bottom inset: Data from inelastic neutron scattering experiments plotted in the same x-y scale. Triangles (yellow) are measured in a direction differing by a reciprocal lattice vector. Rhombuses (orange) are the weaker cross section.

**6. Temperature dependent electronic structures, and atomistic modeling of the negative thermal expansion of  $\delta$  Pu.** Proximity to the localization-delocalization boundary results in strong temperature dependence of the electronic structures of strongly correlated materials. In this task, we incorporated this effect by introducing a phenomenological temperature-dependent parameterization of the modified embedded-atom method. We combined this model with molecular dynamics to simulate the diverse physical properties of the delta and epsilon phases of elemental plutonium. The new model improves upon earlier studies, it captures the negative thermal expansion and the strong temperature dependence of the bulk modulus in the delta phase. We traced this improvement to a strong softening of phonons near the zone boundary and an increase of the f-like partial density and anharmonic effects induced by the temperature-dependent parameterization upon increasing temperature. Publication 9 has resulted from this research.

## IV. SUMMARY

The objective of this research was to develop a method for computational design of modern nuclear fuels whose physical and thermophysical properties can be predicted from first principles using a novel dynamical mean field method for electronic structure calculations. We concentrated our study on a variety of materials ranging from 4f-electron Cerium compounds to elemental plutonium, americium, uranium and plutonium oxides, nitrides, carbides, binary alloys. We addressed the issues connected to their electronic structure, lattice instabilities, phonon and magnon dynamics as well as thermal conductivity. This allowed us to develop new methods, algorithms, and computer codes to evaluate properties of f-electron materials using simulations which avoids costly experiments.

Our major milestone description is as follows:

<b>Milestone Description</b>	<b>Planned Completion Date</b>	<b>Actual Completion Date</b>	<b>Percent Complete</b>
<i>Developments of Novel Electronic Structure Tools for f electron systems</i>	9/30/2013	9/30/2013	100
<i>Applications to Electronic Structure Calculations of Uranium and Cerium Compounds</i>	9/30/2013	9/30/2013	100
<i>Computations of electron and lattice contributions to thermal conductivity in nuclear fuel materials</i>	9/30/2013	9/30/2013	100